Organic & Biomolecular Chemistry

ROYAL SOCIETY OF CHEMISTRY

PAPER

View Article Online
View Journal | View Issue

Cite this: *Org. Biomol. Chem.*, 2025, **23**, 9936

Harnessing the reactivity of captodative radicals: photocatalytic α-pyridination of glycyl derivatives through reversible radical coupling†

Ken Yamazaki, * Shuta Akimoto and Tomoya Miura *

Received 25th April 2025,
Accepted 9th June 2025

DOI: 10.1039/d5ob00675a

rsc.li/obc

Captodative radicals that are highly stabilized by the presence of both electron-donating and electron-withdrawing groups exhibit unique reactivity in organic syntheses. These radicals are known to be less reactive towards radical–radical coupling reactions due to the presence of a shielding occupied molecular orbital. Herein we describe a photocatalytic synthetic strategy for the coupling of two different captodative radicals, which are generated from glycyl derivatives and 4-cyanopyridines. An aromatization is incorporated as the driving force after a reversible radical–radical coupling process. This method can be applied to a wide variety of peptides, providing pharmaceutically relevant pyridyl-functionalized products under mild reaction conditions.

Introduction

Radical–radical coupling reactions represent a keystone in modern synthetic chemistry due to their ability to construct complex molecular architectures with high efficiency and selectivity.[1] The importance of these transformations lies in their capacity to form diverse covalent bonds under mild conditions, thus offering expedient access to a wide array of organic compounds with significant synthetic utility. Among the myriads of radical coupling processes, bond formations between two different radicals stand out as a particularly versatile and powerful strategy, and they can offer an opportunity for the construction of intricate molecular frameworks with unparalleled precision. The formation of a covalent bond between radical species occurs through the overlap of singly occupied molecular orbitals (SOMOs), leading to the sharing of electrons and the establishment of a stable chemical bond.[2] This process relies on the inherent reactivity of radicals, which possess unpaired electrons, making them highly reactive species capable of participating in bond-forming events. The reactivity of radicals is intricately linked to their radical character, which can be categorized into two main classes: persistent radicals, characterized by the longevity of their unpaired electron, and transient radicals, which exhibit a more fleeting nature.[3]

Since Dewar's report in 1952, a fascinating subset of radicals—known as captodative radicals—has garnered significant attention in recent years due to their unique electronic structure and reactivity profile (Scheme 1A).[4] Captodative radicals are characterized by the presence of both electron-donating (captan) and electron-withdrawing (dative) substituents in their molecular framework, resulting in a delicate balance of electronic effects. This electronic arrangement endows captodative radicals with enhanced stability and reactivity, rendering them promising intermediates for their synthetic applications. Intriguingly, the interaction between two captodative radicals offers a rich and unexplored landscape of reactivity, characterized by reversible bond formation and cleavage processes. These radicals have been known for decades, such as **II** and **IV** that can be observed by the bond dissociation from **I** and **V**, respectively. Recently, Bickelhaupt *et al.* proposed that this unique behavior stems from the proximity of the highest occupied molecular orbital (HOMO) to the SOMO in captodative radicals, which acts as a shielding effect with other radicals due to the Pauli repulsion, thereby facilitating the bond cleavage of two radicals (Scheme 1B).[5] Consequently, the controlled manipulation of captodative radical reactivity represents an enticing avenue for the development of novel synthetic methodologies and the construction of complex molecular architectures.

Motivated by the unique reactivity profile of captodative radicals and their potential synthetic applications, we sought to explore the feasibility of harnessing their reactivity in radical–radical coupling between two different captodative rad-

Division of Applied Chemistry, Okayama University, Tsushimanaka, Okayama 700-8530, Japan. E-mail: k-yamazaki@okayama-u.ac.jp, tmiura@okayama-u.ac.jp

†Electronic supplementary information (ESI) available. CCDC 2388516 and 2389158. For ESI and crystallographic data in CIF or other electronic format see DOI: https://doi.org/10.1039/d5ob00675a

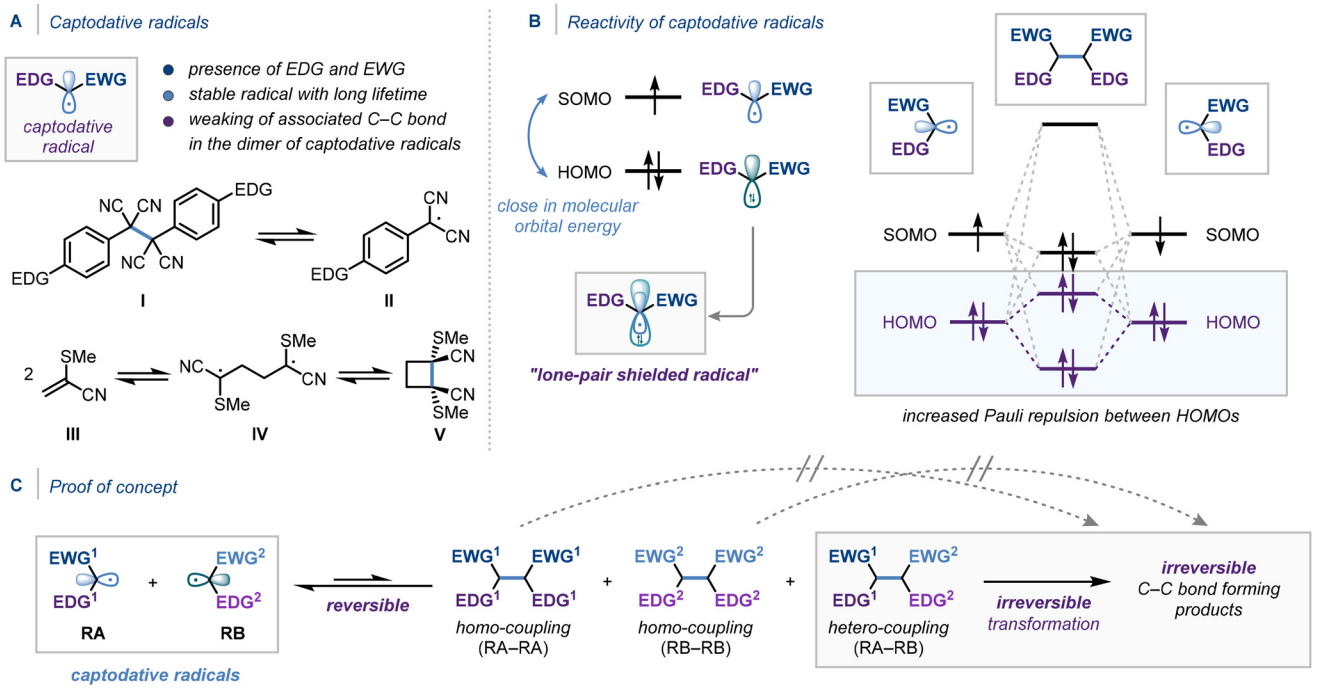

Scheme 1 Captodative radicals and their reactivity. (A) Characteristic features of captodative radicals. (B) Origin of the captodative effect.[5] (C) Synthetic strategy for the hetero-coupling of two captodative radicals.

icals and to devise strategies for controlling their interaction in the context of radical coupling processes. By incorporating additional factors that drive bond formation between two different captodative radicals, we aimed to unlock new avenues for the controlled synthesis of organic molecules with tailored properties and functionalities (Scheme 1C). In this paper, we describe a photocatalytic synthetic strategy for the coupling of two different captodative radicals that incorporates an aromatization as the driving force after a reversible radical–radical coupling process.[6] This method can be applied to a variety of peptides as the captodative radical precursors.

Results and discussion

Among a variety of captodative radicals known to date, we chose glycyl radical and pyridyl radical as the model system in this study.[7–10] The glycyl radical is derived from *N*-phenylglycine ethyl ester (**1a**) (E_p^{ox} = +0.31 V *vs.* SCE in MeCN),[11] while the pyridyl radical originates from 4-cyanopyridine (**2a**) ($E_{1/2}^{red}$ = −1.75 V *vs.* SCE in MeCN),[12] providing a diverse yet synergistic pair for our investigation. The radical cation **A** can be easily obtained through the single electron oxidation of glycine derivative **1a**, while **C** is generated by the single electron reduction of 4-cyanopyridine (**2a**). The balanced redox processes are extremely important for achieving the selective hetero-coupling reaction as overly formed radicals through uncontrolled conditions may result in the homo-coupling of the same radicals.

A proof of concept for this study was to demonstrate the selective coupling of captodative radicals **B** and **D**, while avoiding homo-coupling reactions. To achieve this, we designed the reaction with an aromatization that follows the radical–radical hetero-coupling. This strategy leverages the thermodynamic stability provided by the aromatic product, which drives the reaction towards the desired hetero-coupled product through a radical sorting.[13] We designed the reaction system using the Ir(ppy)$_3$ as a photocatalyst ($E^{\circ}[Ir^{III}*/Ir^{II}]$ = +0.31 V *vs.* SCE, $E^{\circ}[Ir^{II}/Ir^{III}]$ = −2.19 V *vs.* SCE),[14] which possesses sufficient redox potential to facilitate both the oxidation of glycine derivative **1a** and the reduction of 4-cyanopyridine (**2a**). In combination with DABCO (1,4-diazabicyclo[2.2.2]octane) as a base, this system not only promoted the formation of captodative radicals **B** and **D** but also facilitates the rearomatization step. Through a series of optimization experiments, we optimized the reaction conditions to furnish the hetero-coupled product **3a** in 78% (Scheme 2A). Notably, under these conditions, no formation of potential homo-coupled products was detected, underscoring the high selectivity of our reaction system. Furthermore, an addition of TEMPO or BHT to the standard conditions inhibited the product formation (see the ESI†), indicating that a radical is likely to be involved in the reaction pathway (Scheme 2B). When ethyl 2-(phenylimino)acetate **1a′** was used instead of **1a**, no reaction was observed, indicating that **1a′** was not involved in the reaction pathway. Stern–Volmer fluorescence quenching studies revealed that *N*-phenylglycine derivative **1a** is a better quencher of the excited iridium species.

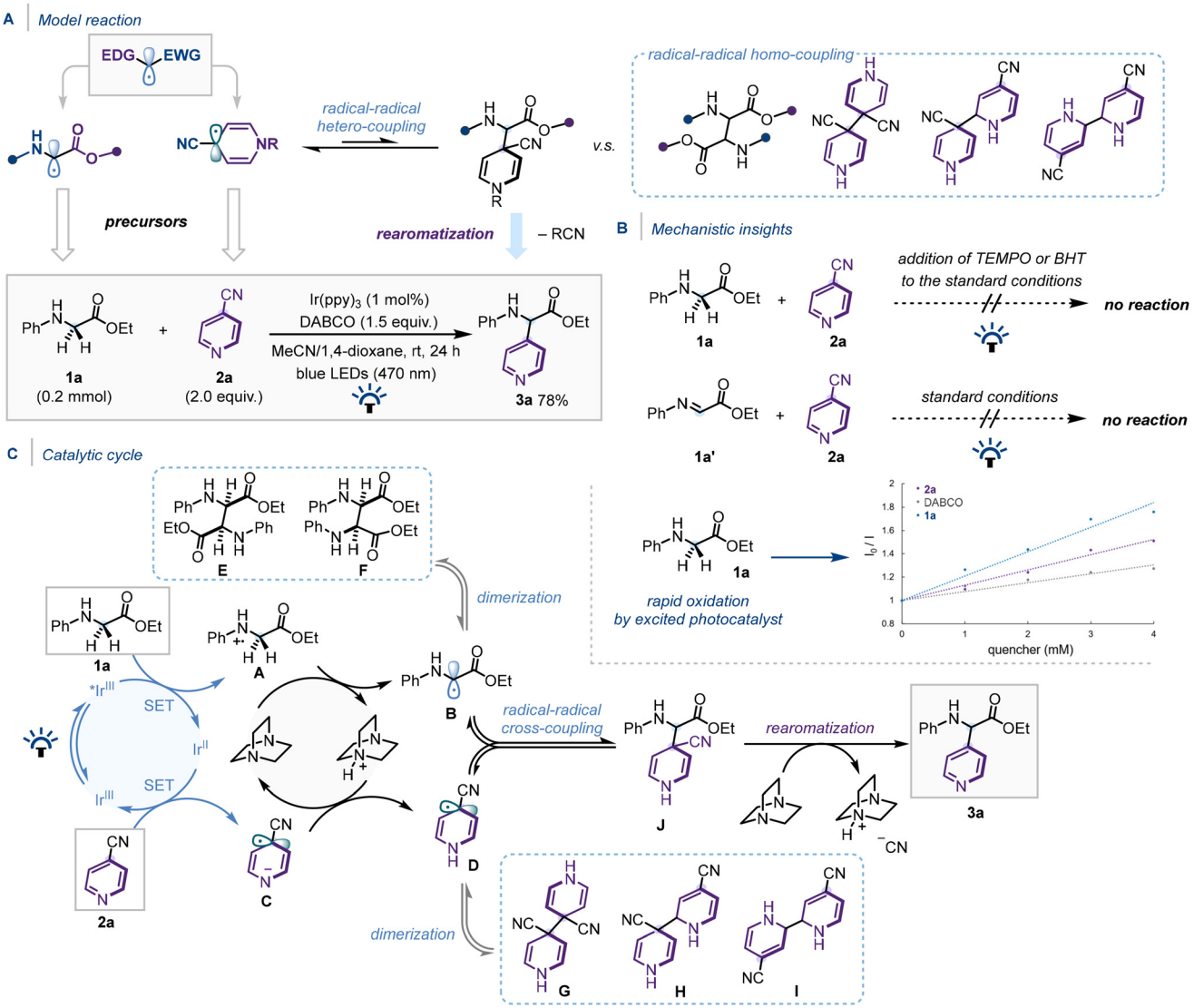

Scheme 2 (A) Model reaction in the radical–radical hetero-coupling of two captodative radials. (B) Mechanistic studies. (C) Proposed reaction mechanism.

Based on the above observations and analyses, we hypothesized the following reaction mechanism (Scheme 2C). Initially, the Ir(ppy)$_3$ photocatalyst is excited by visible light irradiation (470 nm). The excited state Ir* then oxidizes the glycine derivative **1a** through a single electron transfer (SET) to produce a cation radical **A** and the reduced form of Ir(II) photocatalyst.[15] The cation radical **A** is readily deprotonated at the α-position by DABCO, resulting in the formation of a captodative radical **B**. Concurrently, 4-cyanopyridine (**2a**) is reduced by Ir(II) through another SET process, furnishing an anion radical **C** and regenerating the photocatalyst.[16] The anion radical **C** undergoes facile protonation by the protonated base to form another captodative radical **D**. These persistent radicals, **B** and **D**, have the potential to undergo homo-coupling (forming products **E** or **F** from **B**, and **G**, **H**, or **I** from **D**) or hetero-coupling (forming product **J**). Throughout the reversible radical coupling and dissociation of **B** and **D**, the presence of DABCO promotes a smooth rearomatization leading to the formation of the desired product **3a**.

After establishing the optimal reaction conditions and understanding of detailed reaction mechanism for the model reaction, we proceeded to explore the scope of our coupling strategy of two different captodative radicals. We found that a variety of aromatic glycine derivatives **1** worked well in the reaction with **2a** (Scheme 3). *N*-Arylglycine derivatives **1b–1e** possessing *para*-substituents such as methyl and halides gave the desired products **3b–3e** in high yields. However, the reaction of **1f** possessing an electron-withdrawing (CF_3) group was sluggish to give **3f** in a low yield. Interestingly, the *para*-methoxyphenyl (PMP)-substituted substrate **1g** furnished the product **3g** in 39% yield under the standard conditions along with the undesired *N*-pyridinated byproduct **3g′** in 28% yield

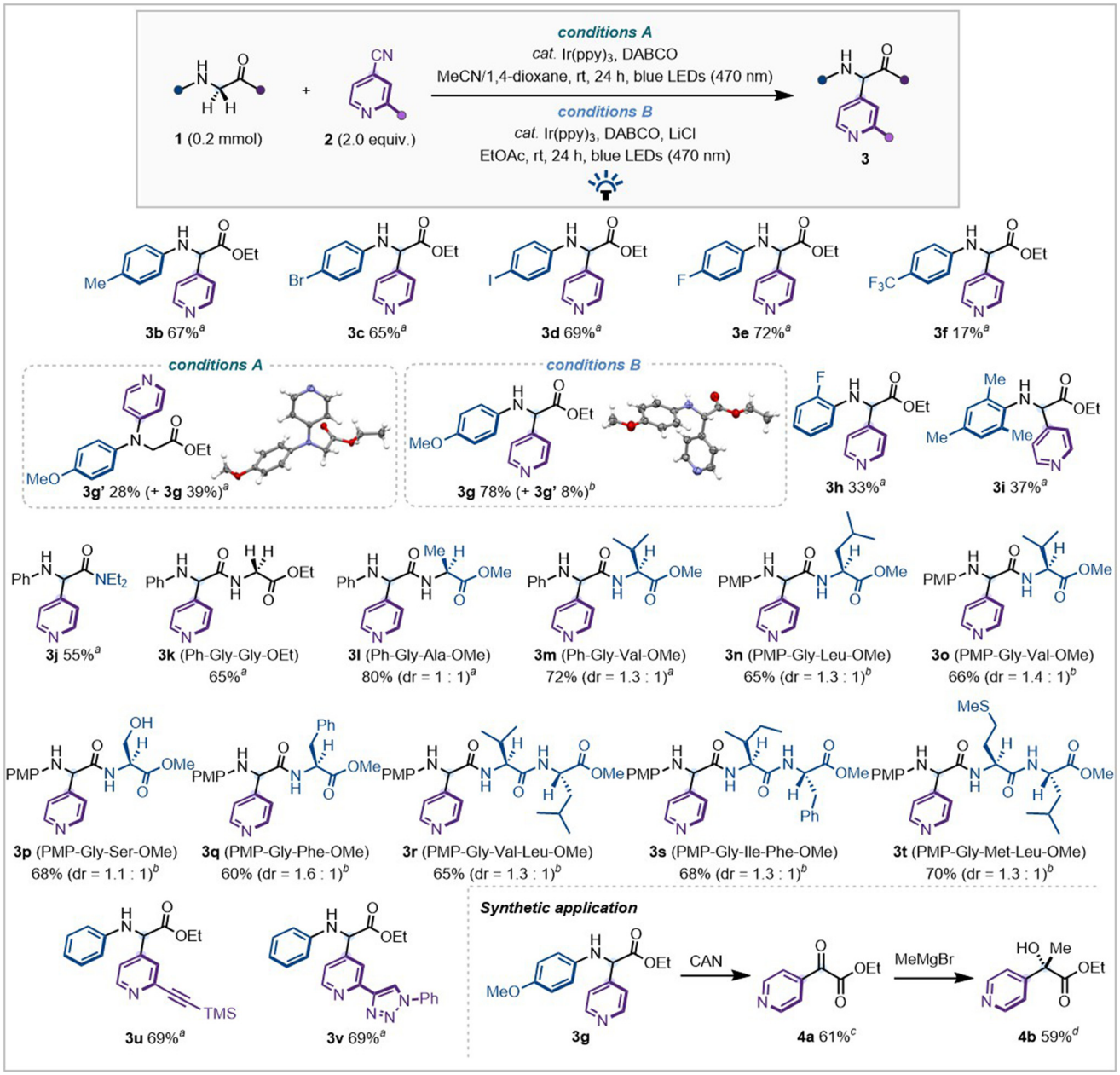

Scheme 3 Substrate scope of the pyridination of glycine derivatives. [a] Conditions A: **1** (0.2 mmol, 1.0 equiv.), **2** (2.0 equiv.), $Ir(ppy)_3$ (1.0 mol%), DABCO (1.5 equiv.), MeCN/1,4-dioxane (0.10 M), rt, 24 h, blue LEDs (470 nm). [b] Conditions B: **1** (0.2 mmol, 1.0 equiv.), **2** (2.0 equiv.), $Ir(ppy)_3$ (1.0 mol%), DABCO (2.5 equiv.), LiCl (1.2 equiv.), EtOAc (0.067 M), rt, 24 h, blue LEDs (470 nm). [c] **3g** (0.6 mmol, 1.0 equiv.), CAN (2.2 equiv.), MeCN/H_2O (0.10 M), rt, 2 h. [d] **4a** (0.10 mmol, 1.0 equiv.), MeMgBr (2.0 equiv.), THF (0.050 M), 0 °C to rt, 17 h.

(see the ESI†). Pleasingly, we were successfully able to control the reaction between an *in situ*-generated captodative radicals from the starting material **1g** and 4-cyanopyridine (**2a**) by the addition of LiCl additive, and the modified conditions greatly suppressed the formation of byproduct **3g′** to provide the desired compound **3g** in 78% yield. The introduction of *ortho*-substituents **1h** and **1i** resulted in diminished yields. Additionally, a substrate **1j** with *tert*-amide substituent gave the pyridinated product **3j** in 55% yield. Notably, our method is not limited to the glycine derivatives alone, but also applicable to a variety of peptides under the standard conditions. Dipeptides bearing glycine (**1k**), alanine (**1l**), valine (**1m**), leucine (**1n**), valine (**1o**), serine (**1p**), and phenylalanine (**1q**) ethyl esters with glycine N-terminus (Ph- or PMP-) were well tolerated to give the corresponding products **3k–3q** in good to high yields. Subjecting tripeptides **1r–1t** also furnished the desired products **3r–3t** in good yields. In every example, we observed no trace of epimerization of the products from the enantiomerically pure starting materials. The other captodative radical precursor is not only limited to 4-cyanopyridine (**2a**),

and we have found that the presence of silylated alkynyl or heterocycle adjacent to the pyridine nitrogen atom does not affect the reactivity to give the products **3u** and **3v** in 69% yields, respectively. The trace amount of *N*-pyridinated byproducts were observed in most examples under Conditions B.

The synthetic utility of the products was demonstrated by the further transformations of **3g**. The amine protecting PMP group was converted into carbonyl group, giving α-keto ester **4a** in 61% yield when a simple oxidation protocol using ceric ammonium nitrate (CAN) was applied. α-Hydroxy ester **4b** was obtained on the treatment of **4a** with MeMgBr.

Conclusions

A photocatalytic synthetic strategy for the radical–radical coupling reaction between two captodative radicals was developed. An aromatization was successfully incorporated as the driving force after a reversible C–C bond forming coupling process to selectively furnish a wide variety of pyridyl-functionalized products in high yields. Our findings and the mechanistic investigation not only expand the synthetic toolbox available to chemists but also pave the way for the development of innovative strategies for the bond formation and functionalization in organic synthesis.

Data availability

The data supporting this article have been included as part of the ESI.†

Conflicts of interest

There are no conflicts to declare.

Acknowledgements

This work was supported in part by JSPS KAKENHI [Grants-in-Aids for Transformative Research Areas (A) (22H05368, 24H01083, 24H01861), Challenging Exploratory Research (22K19032), Early-Career Scientists (24K17682)], Chugai Foundation for Innovative Drug Discovery Science: C-FINDs, Astellas Foundation for Research on Metabolic Disorders, and Takeda Science Foundation.

References

1 (*a*) K. L. Skubi, T. R. Blum and T. P. Yoon, *Chem. Rev.*, 2016, **116**, 10035; (*b*) J. Xie, H. Jin and A. S. K. Hashmi, *Chem. Soc. Rev.*, 2017, **46**, 5193; (*c*) H. Yi, G. Zhang, H. Wang, Z. Huang, J. Wang, A. K. Singh and A. Lei, *Chem. Rev.*, 2017, **117**, 9016; (*d*) J. Xie, H. Jin and A. S. K. Hashmi, *Chem. Soc. Rev.*, 2017, **46**, 5193; (*e*) L. Marzo, S. K. Pagire, O. Reiser and B. König, *Angew. Chem., Int. Ed.*, 2018, **57**, 10034; (*f*) R. S. J. Proctor and R. J. Phipps, *Angew. Chem., Int. Ed.*, 2019, **58**, 13666; (*g*) G. E. M. Crisenza, D. Mazzarella and P. Melchiorre, *J. Am. Chem. Soc.*, 2020, **142**, 5461; (*h*) X.-Y. Yu, Q.-Q. Zhao, J. Chen, W.-J. Xiao and J.-R. Chen, *Acc. Chem. Res.*, 2020, **53**, 1066; (*i*) A. Péter, S. Agasti, O. Knowles, E. Pye and D. J. Procter, *Chem. Soc. Rev.*, 2021, **50**, 5349; (*j*) J. D. Bell and J. A. Murphy, *Chem. Soc. Rev.*, 2021, **50**, 9540.

2 (*a*) H. Tanaka, *Prog. Polym. Sci.*, 2003, **28**, 1171; (*b*) E. V. Anslyn and D. A. Dougherty, *Modern Physical Organic Chemistry*, University Science Books, Sausalito, 2006; (*c*) J. Clayden, N. Greeves and S. Warren, *Organic Chemistry, 2nd ed*, Oxford University Press, Oxford, 2012; (*d*) D. Cambié, C. Bottecchia, N. J. W. Straathof, V. Hessel and T. Noël, *Chem. Rev.*, 2016, **116**, 10276; (*e*) S. Yasuda, T. Ishii, S. Takemoto, H. Haruki and H. Ohmiya, *Angew. Chem., Int. Ed.*, 2018, **57**, 2938; (*f*) J. Autschbach, *Quantum Theory for Chemical Applications: From Basic Concepts to Advanced Topics*, Oxford University Press, 2020; (*g*) T. Ishii, K. Nagao and H. Ohmiya, *Chem. Sci.*, 2020, **11**, 5630; (*h*) H. Ohmiya, *ACS Catal.*, 2020, **10**, 6862; (*i*) J. A. P. Maitland, J. A. Leitch, K. Yamazaki, K. E. Christensen, D. J. Cassar, T. A. Hamlin and D. J. Dixon, *Angew. Chem., Int. Ed.*, 2021, **60**, 24116; (*j*) S. Kasemthaveechok, L. Abella, J. Crassous, J. Autschbach and L. Favereau, *Chem. Sci.*, 2022, **13**, 9833; (*k*) J. Zhang and M. Rueping, *Chem. Soc. Rev.*, 2023, **52**, 4099; (*l*) J. J. A. Garwood, A. D. Chen and D. A. Nagib, *J. Am. Chem. Soc.*, 2024, **146**, 28034; (*m*) J. Zhang and M. Rueping, *Nat. Catal.*, 2024, **7**, 963; (*n*) Y. Hordijk, M. Dalla Tiezza, D. Rodrigues Silva and T. A. Hamlin, *ChemPhysChem*, 2025, **26**, e202400728.

3 (*a*) H. Fischer, *Chem. Rev.*, 2001, **101**, 3581; (*b*) K. J. Romero, M. S. Galliher, D. A. Pratt and C. R. J. Stephenson, *Chem. Soc. Rev.*, 2018, **47**, 7851; (*c*) D. Leifert and A. Studer, *Angew. Chem., Int. Ed.*, 2020, **59**, 74.

4 (*a*) M. J. S. Dewar, *J. Am. Chem. Soc.*, 1952, **74**, 3353; (*b*) R. W. Baldock, P. Hudson, A. R. Katritzky and F. Soti, *J. Chem. Soc., Perkin Trans. 1*, 1974, 1422; (*c*) L. Stella, Z. Janousek, R. Merényi and H. G. Viehe, *Angew. Chem., Int. Ed. Engl.*, 1978, **17**, 691; (*d*) H. G. Viehe, R. Merényi, L. Stella and Z. Janousek, *Angew. Chem., Int. Ed. Engl.*, 1979, **18**, 917; (*e*) D. Crans, T. Clark and P. von Ragué Schleyer, *Tetrahedron Lett.*, 1980, **21**, 3681; (*f*) M. Klessinger, *Angew. Chem., Int. Ed. Engl.*, 1980, **19**, 908; (*g*) H. G. Viehe, Z. Janousek, R. Merényi and S. Stella, *Acc. Chem. Res.*, 1985, **18**, 148.

5 E. Blokker, M. ten Brink, J. M. van der Schuur, T. A. Hamlin and F. M. Bickelhaupt, *ChemistryEurope*, 2023, **1**, e202300006.

6 During the preparation of this manuscript, the similar radical-radical coupling reactions using 3CzIPN as the photoredox catalyst was disclosed by Pan and Yu: C. Pan, D. Chen, Y. Cheng and J.-T. Yu, *Chem. Commun.*, 2024, **60**,

4451. See also: X.-C. Cui, H. Zhang, H. Zhang, Y.-P. Wang, J.-P. Qu and Y.-B. Kang, *Org. Lett.*, 2023, **25**, 7198.

7 For selected reviews on the radical-mediated functionalization of glycine derivatives, see: (*a*) J. Xie, H. Jin, P. Xu and C. Zhu, *Tetrahedron Lett.*, 2014, **55**, 36; (*b*) M. H. Babu and J. Sim, *Eur. J. Org. Chem.*, 2022, e202200859; (*c*) Y. Tian, X. Bu, Y. Chen, L. Wang, J. E, J. Zeng, H. Xu, A. Han, X. Yang and Z. Zhao, *Catalysts*, 2023, **13**, 1502; (*d*) A. M. Yousif, S. Colarusso and E. Bianchi, *Eur. J. Org. Chem.*, 2023, e202201274; (*e*) C. Wang, R. Qi, R. Wang and Z. Xu, *Acc. Chem. Res.*, 2023, **56**, 2110.

8 For selected examples of the photoinduced functionalization of glycine derivatives, see: (*a*) S. Zhu and M. Rueping, *Chem. Commun.*, 2012, **48**, 11960; (*b*) J. Xuan, T.-T. Zeng, Z.-J. Feng, Q.-H. Deng, J.-R. Chen, L.-Q. Lu, W.-J. Xiao and H. Alper, *Angew. Chem., Int. Ed.*, 2015, **54**, 1625; (*c*) X.-W. Gao, Q.-Y. Meng, J.-X. Li, J.-J. Zhong, T. Lei, X.-B. Li, C.-H. Tung and L.-Z. Wu, *ACS Catal.*, 2015, **5**, 2391; (*d*) C. Wang, R. Qi, H. Xue, Y. Shen, M. Chang, Y. Chen, R. Wang and Z. Xu, *Angew. Chem., Int. Ed.*, 2020, **59**, 7461; (*e*) L. Leng and J. M. Ready, *ACS Catal.*, 2020, **10**, 13196; (*f*) R. Qi, C. Wang, Y. Huo, H. Chai, H. Wang, Z. Ma, L. Liu, R. Wang and Z. Xu, *J. Am. Chem. Soc.*, 2021, **143**, 12777; (*g*) C. Che, Y.-N. Li, X. Cheng, Y.-N. Lu and C.-J. Wang, *Angew. Chem., Int. Ed.*, 2021, **60**, 4698; (*h*) J. Wang, Y. Ye, T. Sang, C. Zhou, X. Bao, Y. Yuan and C. Huo, *Org. Lett.*, 2022, **24**, 7577; (*i*) R. Qi, C. Wang, Z. Ma, H. Wang, Q. Chen, L. Liu, D. Pan, X. Ren, R. Wang and Z. Xu, *Angew. Chem., Int. Ed.*, 2022, **61**, e202200822; (*j*) Y.-N. Ding, N. Li, Y.-C. Huang, Y. An and Y.-M. Liang, *Org. Lett.*, 2022, **24**, 4519; (*k*) J. Tan, L. Yang, H. Su, Y. Yang, Z. Zhong, X. Feng and X. Liu, *Chem. Sci.*, 2024, **15**, 16050; (*l*) F. Yang, L. Chi, Z. Ye and L. Gong, *J. Am. Chem. Soc.*, 2025, **147**, 1767.

9 For selected reviews on the radical-mediated functionalization of 4-cyanopyridine, see: (*a*) J.-M. R. Mattalia, *Beilstein J. Org. Chem.*, 2017, **13**, 267; (*b*) S. Tong, K. Li, X. Ouyang, R. Song and J. Li, *Green Synth. Catal.*, 2021, **2**, 145; (*c*) J. Huang and Z. Chen, *Adv. Synth. Catal.*, 2023, **365**, 2058; (*d*) F. Chao, H.-B. Yang and Y. Fang, *ChemCatChem*, 2024, **16**, e202301281.

10 For selected examples of the photoinduced functionalization of 4-cyanopyridine, see: (*a*) A. McNally, C. K. Prier and D. W. C. MacMillan, *Science*, 2011, **334**, 1114; (*b*) M. T. Pirnot, D. A. Rankic, D. B. C. Martin and D. W. C. MacMillan, *Science*, 2013, **339**, 1593; (*c*) Z. Zuo and D. W. C. MacMillan, *J. Am. Chem. Soc.*, 2014, **136**, 5257; (*d*) J. D. Cuthbertson and D. W. C. MacMillan, *Nature*, 2015, **519**, 74; (*e*) F. Lima, M. A. Kabeshov, D. N. Tran, C. Battilocchio, J. Sedelmeier, G. Sedelmeier, B. Schenkel and S. V. Ley, *Angew. Chem., Int. Ed.*, 2016, **55**, 14085; (*f*) K. Nakajima, S. Nojima, K. Sakata and Y. Nishibayashi, *ChemCatChem*, 2016, **8**, 1028; (*g*) G. Wang, H. Zhang, J. Zhao, W. Li, J. Cao, C. Zhu and S. Li, *Angew. Chem., Int. Ed.*, 2016, **55**, 5985; (*h*) G. Wang, J. Cao, L. Gao, W. Chen, W. Huang, X. Cheng and S. Li, *J. Am. Chem. Soc.*, 2017, **139**, 3904; (*i*) Y. Deng, Q. Liu and A. B. Smith, III, *J. Am. Chem. Soc.*, 2017, **139**, 9487; (*j*) M. M. Walker, B. Koronkiewicz, S. Chen, K. N. Houk, J. M. Mayer and J. A. Ellman, *J. Am. Chem. Soc.*, 2020, **142**, 8194; (*k*) T. Nakashima, H. Fujimori, K. Ohmatsu and T. Ooi, *Chem. – Eur. J.*, 2021, **27**, 9253; (*l*) J. Shi, T. Yuan, M. F. Zheng and X. Wang, *ACS Catal.*, 2021, **11**, 3040; (*m*) F. Kobayashi, M. Fujita, T. Ide, Y. Ito, K. Yamashita, H. Egami and Y. Hamashima, *ACS Catal.*, 2021, **11**, 82; (*n*) H. Li and S. Chiba, *Chem. Catal.*, 2022, **2**, 1128; (*o*) X.-C. Cui, H. Zhang, Y.-P. Wang, J.-P. Qu and Y.-B. Kang, *Chem. Sci.*, 2022, **13**, 11246.

11 C. Wang, M. Guo, R. Qi, Q. Shang, Q. Liu, S. Wang, L. Zhao, R. Wang and Z. Xu, *Angew. Chem., Int. Ed.*, 2018, **57**, 15841.

12 C. P. Andrieux, L. Gelis, M. Medebielle, J. Pinson and J. M. Saveant, *J. Am. Chem. Soc.*, 1990, **112**, 3509.

13 (*a*) W. Liu, M. N. Lavagnino, C. A. Gould, J. Alcázar and D. W. C. MacMillan, *Science*, 2021, **374**, 1258; (*b*) H. A. Sakai and D. W. C. MacMillan, *J. Am. Chem. Soc.*, 2022, **144**, 6185; (*c*) A. V. Tsymbal, L. D. Bizzini and D. W. C. MacMillan, *J. Am. Chem. Soc.*, 2022, **144**, 21278; (*d*) J. Z. Wang, E. Mao, J. A. Nguyen, W. L. Lyon and D. W. C. MacMillan, *J. Am. Chem. Soc.*, 2024, **146**, 15693; (*e*) R. Chen, N. E. Intermaggio, J. Xie, J. A. Rossi-Ashton, C. A. Gould, R. T. Martin, J. Alcázar and D. W. C. MacMillan, *Science*, 2024, **383**, 1350.

14 I. M. Dixon, J.-P. Collin, J.-P. Sauvage, L. Flamigni, S. Encinas and F. Barigelletti, *Chem. Soc. Rev.*, 2000, **29**, 385.

15 Although the Stern–Volmer plot indicates that the excited state $Ir(ppy)_3$ is likely quenched by **1a** in the photocatalytic cycle, a smaller yet measurable slope observed with **2a** suggests that an alternative reductive quenching pathway may also be operative.

16 F. Chao, H.-B. Yang and Y. Fang, *ChemCatChem*, 2024, **16**, e202301281.